

# Micromachined Low-Loss Microwave Switches

Z. Jamie Yao, Shea Chen, Susan Eshelman, David Denniston, *Associate Member, IEEE*,  
and Chuck Goldsmith, *Senior Member, IEEE*

**Abstract**—The design and fabrication of a micromechanical capacitive membrane microwave switching device is described. The switching element consists of a thin metallic membrane, which has two states, actuated or unactuated, depending on the applied bias. A microwave signal is switched on and off when the membrane is switched between the two states. These switches have a switching on speed of less than 6  $\mu$ s and a switching off speed of less than 4  $\mu$ s. The switching voltage is about 50 V. The switches have a bowtie shape and showed low insertion loss of 0.14 dB at 20 GHz and 0.25 dB at 35 GHz, and isolation of 24 dB at 20 GHz and 35 dB at 35 GHz. These devices offer the potential for building a new generation of low-loss high-linearity microwave circuits for a variety of phased antenna arrays for radar and communications applications. [324]

**Index Terms**—Capacitive switches, low loss, microwave, RFMEMS, surface micromachining.

## I. INTRODUCTION

DEVELOPMENTS in MEMS technology have made possible the design and fabrication of control devices suitable for switching microwave signals. Micromechanical switches were first demonstrated in 1979 [1] as electrostatically actuated cantilever switches used to switch low-frequency electrical signals. Since then, these switches have demonstrated useful performance at microwave frequencies using cantilever [2], [3], rotary [4], and membrane topologies [5], [6]. These switches have shown that moving metal contacts possess low parasitics at microwave frequencies (due to their small size) and are amenable to achieving low on-resistance (resistive switching) or high on-capacitance (capacitive switching).

Micromechanical membrane switches have several advantages compared to FET or p-i-n diode switches. Eliminating the use of semiconductor p-n and metal-semiconductor junctions in radio frequency (RF) devices serves three very useful functions. First, the contact and spreading resistance associated with ohmic contacts are eliminated, significantly reducing the resistive losses in the device. Instead, high conductivity films are used to fabricate metal structures that carry RF currents with ultra-low losses. Second, the removal of  $I$ - $V$  nonlinearities associated with semiconductor junctions significantly improves the distortion characteristics and power handling of the RF MEMS devices. RF MEMS switches exhibit no measurable harmonics or intermodulation distortion. Meanwhile, the power handling of these devices is limited mostly by

Manuscript received January 30, 1998; revised January 7, 1999. This work was supported by DARPA under Contract N66001-96-C-8623. Subject Editor, J. Fluitman.

The authors are with the RF/Microwave Laboratory, Raytheon Systems Company, Dallas, TX 75243 USA (e-mail: z-yao1@raytheon.com).

Publisher Item Identifier S 1057-7157(99)04265-1.

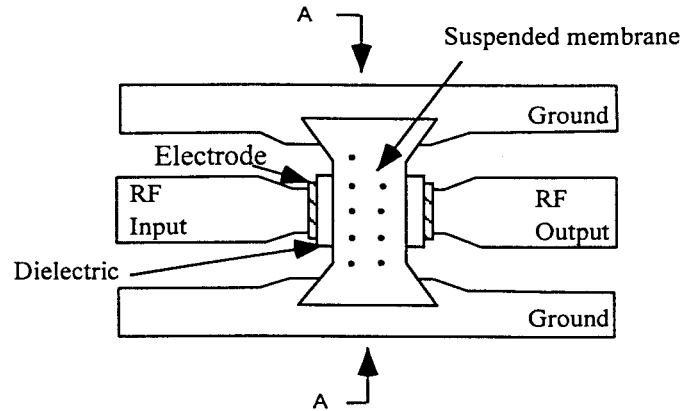


Fig. 1. Schematic of top view of a shunt micromechanical switch.

current density limitations. Third, electrostatic operation of the mechanical motion of the RF MEMS devices requires negligible quiescent current consumption. Typical switching energy is approximately 10 nJ. The main limitation of these switches is their switching speed. Microsecond switching precludes their use in high-speed applications such as transmit/receive switching. However, these speeds are more than sufficient for a variety of applications including beam steering in phased antenna arrays. This paper describes significant improvements to the design of metal membrane switches which operate with significantly reduced losses, increased operating frequencies, and improved switching speeds over previously reported work [5], [6].

## II. CAPACITIVE MEMBRANE SWITCH OPERATION

Typical micromechanical switches utilize the mechanical connection of two metallic surfaces to actuate a low resistance connection. However, in micromechanical switches, the forces of stiction and microwelding are commensurate with the restoring force of the switch. As a result, these switches may operate unreliably or be subject to premature failure. The switches described in this paper have been designed to significantly reduce stiction and eliminate microwelding by replacing the metal-to-metal ohmic contact with a capacitive connection.

The geometry of a capacitive metal membrane shunt switch as described in this paper is shown in Fig. 1 (top view) and Fig. 2 (cross section). The membrane switches described in this paper are about 120  $\mu$ m in width and 280  $\mu$ m in length. The switch consists of a thin metallic membrane suspended over a dielectric film deposited on top of a bottom electrode as shown in Fig. 2(a). When an electrostatic potential is applied between the membrane and the bottom electrode, the attractive

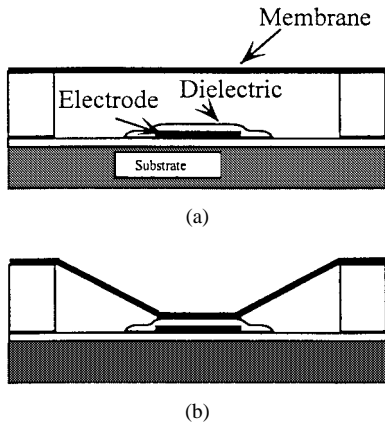


Fig. 2. Schematic of cross section A-A of the switch shown in Fig. 1: (a) switch up and (b) switch down.

electrostatic force pulls the metal membrane down onto the bottom dielectric, as shown in Fig. 2(b). The dielectric film serves to prevent stiction between the two metallic surfaces, yet provides a low impedance path between the two contacts.

When the membrane is unactuated, the air dielectric between the two contacts exhibits a very low capacitance, given by

$$C_{\text{off}} = \frac{1}{\frac{h_D}{\epsilon_D A} + \frac{h_a}{\epsilon_0 A}} \quad (1)$$

where  $C_{\text{off}}$  is the capacitance of the switch in the off state,  $\epsilon_D$  and  $\epsilon_0$  are the dielectric constants of air and dielectric material used,  $h_D$  is the dielectric layer thickness,  $h_a$  is the air gap between the membrane and the dielectric layer when the switch is at the up-position, and  $A$  is the overlap area between the bottom electrode and the membrane. For typical switch dimensions, the off-capacitance is on the order of tens of femtofarads. When the switch is actuated, the metal-dielectric-metal sandwich possesses significant capacitance ( $C_{\text{on}}$ ), described as

$$C_{\text{on}} = \frac{\epsilon_D A}{h_D}. \quad (2)$$

Typical capacitance values for this position are 3–4 pF. The ratio of available on-impedance to off-impedance of the switch is given by the ratio of the on-capacitance to off-capacitance. With proper design of switch geometry and material selection, this ratio can exceed 100, more than sufficient for switching signals at microwave frequencies.

The switch described in this paper was designed to 1) minimize device insertion loss and 2) maximize the on/off ratio of the device. The geometry of the electrode and membrane was chosen to minimize the through-path resistance and achieve an off-capacitance that can be impedance matched to frequencies as high as 40 GHz. The characteristics of the dielectric layer as well as the electrode, membrane, and gap geometry were set to achieve an on/off capacitance ratio of 100. Switch pull-down voltages, dielectric breakdown, and switching speeds also contribute design tradeoffs that must be compromised with RF performance. The switch circuitry

TABLE I  
MICROWAVE SWITCH DEVICE PERFORMANCE COMPARISON

Device Type	$R_{\text{on}}$ (ohms)	$C_{\text{off}}$ (fF)	FOM-Cutoff Freq. (GHz)
GaAs MESFET	2.3	249	280
GaAs pHEMT	4.7	80	420
GaAs p-i-n Diode	5.6	420	730
Metal Membrane Capacitive	0.4	35	>9000

consists of coplanar waveguide (CPW) transmission lines which have an impedance of  $50 \Omega$  that matches the impedance of the system (Fig. 1). The transmission lines are  $120 \mu\text{m}$  in width. The spacing between the ground lines and the signal line is  $80 \mu\text{m}$  (Fig. 1).

In practical switches, the on-impedance of the switch at high frequencies is limited by parasitic resistances contained within the switch. Conversely, the off-impedance of the switch is determined by its off-capacitance. A common measure of performance for electronic switches is the cutoff frequency, the theoretical frequency where the ratio of off-impedance to on-impedance degrades to unity. This frequency is given by

$$f_c = \frac{1}{2\pi R_{\text{on}} C_{\text{off}}} \quad (3)$$

where  $R_{\text{on}}$  is the effective on-resistance, and  $C_{\text{off}}$  is the off-state capacitance of the switch.

The cutoff frequency does not represent a frequency where the switch is operated, but merely a theoretical basis for comparison. Table I shows the figures of merit (FOM) for practical electrical and micromechanical devices which operate at 20 GHz.

Inspection of this data indicates that micromechanical switches possess the potential for significantly improved performance compared to electronic devices. The order of magnitude improvement in figure of merit for RF MEMS switches compared to typical GaAs FET switches means that RF MEMS switches will operate with significantly lower loss and lower parasitics than their electronic counterparts.

### III. FABRICATION

Surface micromachining techniques were utilized to fabricate the switches described in this paper. High resistivity (greater than  $5000 \Omega\text{-cm}$ ) silicon wafers were used as substrates. Fig. 3 shows the essential process steps: 1) One micrometer of insulating thermal oxide was grown on the substrate. 2) A layer of tungsten ( $<0.5 \mu\text{m}$ ) was sputtered and patterned to define the electrodes. 3) A thin layer (less than  $2000 \text{ \AA}$ ) of dielectric (PECVD silicon nitride) is deposited and patterned to insulate the electrodes. The dielectric constant of the nitride is about 6.7. 4) A  $4\text{-}\mu\text{m}$ -thick aluminum layer is evaporated and wet etched using a commercial aluminum etchant to define the transmission lines and the posts for the membranes. All the line widths need to be oversized by  $5 \mu\text{m}$  to compensate for the decrease in line width due to wet etch. 5) A photoresist sacrificial spacer layer is spin coated and patterned. 6) An aluminum alloy membrane layer is sputtered

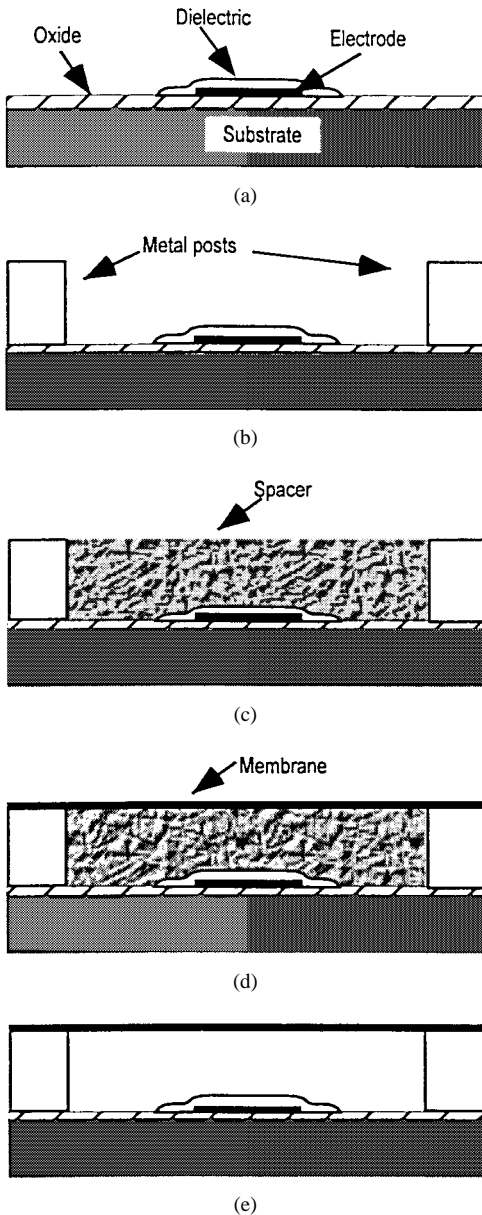


Fig. 3. Schematic illustration of process flow: (a) oxide deposition, electrode, dielectric deposition and patterning; (b) metal posts deposition and patterning; (c) spacer coating and patterning; (d) membrane deposition and patterning; and (e) removal of the spacer by dry etching.

and wet etched. 7) The spacer material is removed by oxygen plasma etch to release the membrane. There are access holes ( $2 \times 2 \mu\text{m}$ ) on the membrane to accelerate the release rate. The total etch time is about 100 min. Fig. 4(a) and (b) shows micrographs of a shunt switch in the (a) off-state and (b) on-state.

#### IV. FABRICATION ISSUES

The fabrication procedures described in this paper are relatively simple. The process requires only five mask layers. The devices can be fabricated on not only high resistivity silicon but also sapphire and GaAs wafers. The devices can be designed with loose geometrical tolerances for high yield processing. Using high resistivity silicon wafers allows

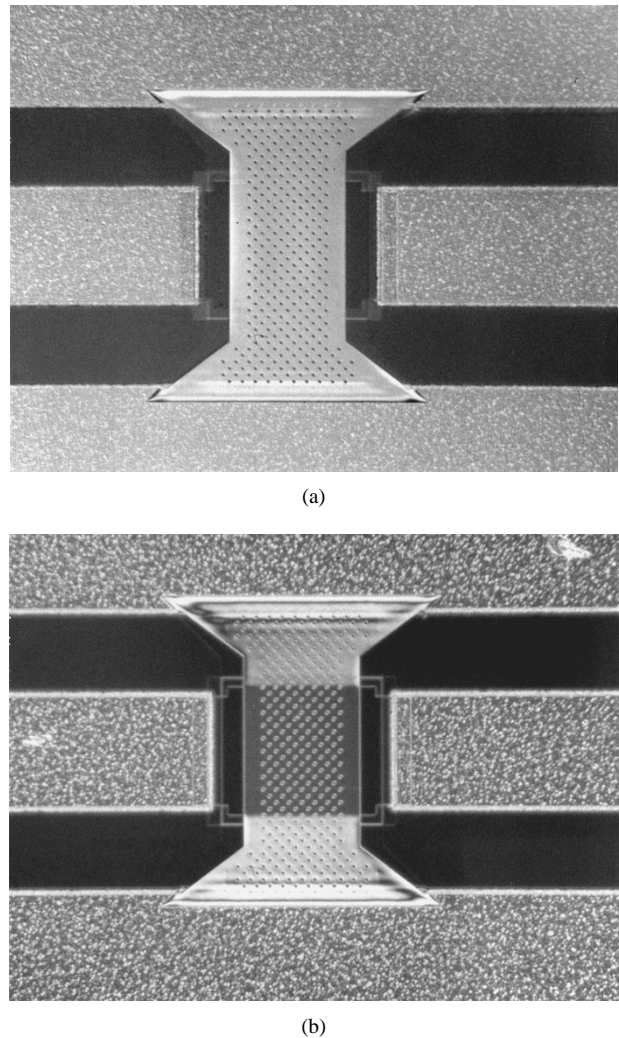


Fig. 4. Micrograph of a RF switch at: (a) up and (b) down positions.

the possibility for integration with CMOS for multifunction assemblies.

There are challenges in fabricating the devices. The gap between the membrane (the top electrode) and the bottom electrode should not be too large. Otherwise the pull down voltage is too high. In order to achieve desired capacitance ratio, 100:1, the membrane down position capacitance needs to be sufficiently high. Therefore, the membrane and the dielectric on top of the electrode need to be in intimate contact. The smaller the air gap between the two surfaces, the higher the capacitance is. There are several factors that limit the contact. One cause of increasing air gap is hillocking. Hillocking occurs if a low melting temperature metallic thin film is exposed to high temperature. In our process, the silicon nitride is deposited at  $300^\circ\text{C}$ . When aluminum is used as the electrode, hillocking occurs. Hillocking can be limited by depositing a layer of metal that has high melting temperature on top of the aluminum. For example, a thin layer of chrome may be deposited on top of the aluminum. This will eliminate the hillocking of the aluminum and the surface remains smooth. To simplify the process, a high melting temperature metal is preferred. Fig. 5 shows an image from atomic force microscopy (AFM) measurement of a smooth

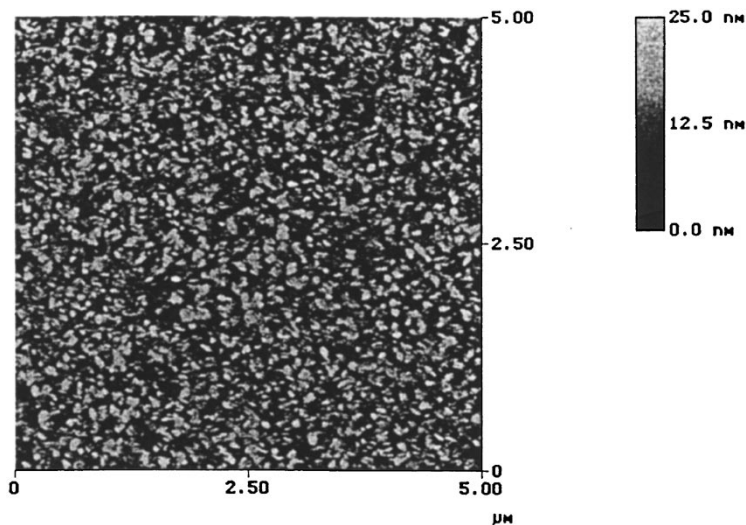


Fig. 5. Atomic force microscopy image of electrode surface.

TABLE II  
SWITCHES' SURFACE ROUGHNESS AND THEIR ON-CAPACITANCE

Roughness, RMS	On-capacitance (pF)
21	2.1
6	3.5

electrode surface. The roughness RMS is about 3.1 nm. It was experimentally determined that high pressure and high power result in a smooth film surface. Another reason that may diminish the intimate contact is the residue left after release etch. Polymer residues can also cause a sticking problem. The wafer temperature is controlled below 150 °C in the etch process. This helps minimize the residue on the top of the dielectric and the bottom of the membrane. The roughness of the surface that is in contact with the membrane during actuation of switches was measured using AFM. The suspended membrane was peeled to expose dielectric film surface prior to measurement. The surface roughness and the switch on-capacitance (membrane actuated position) are listed in Table II. The results indicate that the roughness has significant influence on the switch on-capacitance.

Stresses in a suspended membrane affect the operation of the device. Compressive stress is undesirable since it will cause the membrane to buckle and alter the off capacitance in the unactuated state. High tensile stress is also undesirable since it will increase the pull-down voltage. The optimum situation is low tensile stress. There was no method available to us to measure the residual stress in the suspended membrane. Therefore, the membrane stress as deposited on an unpatterned spacer layer (on a blank wafer) was determined by measuring the radius of curvature of the wafer. The assumption was made that the calculated membrane stress would correlate with the residual stress in the suspended membrane. The membrane stress depends on the deposition conditions, the spacer material, and the membrane material. The stress was controlled at less than 120 MPa by adjusting the power, pressure, and the flow rate of argon. We have experimented with different membrane materials, such as an aluminum/silicon/aluminum sandwich, tungsten, and aluminum alloy. We have also used

different spacer materials, such as polyimide and photoresist. The aluminum alloy combined with photoresist gave the lowest tensile stress.

## V. TEST RESULTS AND DISCUSSIONS

The primary measure of performance for an electronic switch is insertion loss when signals are being passed and isolation when signals are being rejected. The switch shown in Fig. 1 is a shunt switch to ground. When it is unactuated, the RF signal passes underneath the membrane with relatively little attenuation. When the switch is actuated, the metal-dielectric-metal sandwich produces a low impedance path to the surrounding coplanar waveguide grounds. This prevents the RF signal from traversing beyond the switch.

This high-frequency switch possesses approximately 0.15 dB of loss at 10 GHz and 0.28 dB at 35 GHz. Variability of the measurements was approximately  $\pm 0.05$  dB, mainly because of difficulty in making good contact between the probes and aluminum lines due to formation of aluminum oxide. This low insertion loss represents the ohmic losses from the metal conductors for the RF signal as it traverses the switch. Compared with typical FET or p-i-n diode switches, which have insertion loss about 1 dB [7], [8], the micromechanical switches have significant advantages. For a system, such as a time-delay phase shifter, that may require many switches, the total loss is significantly lower when mechanical switches are utilized.

Micromechanical switches possess an excellent impedance match to 50  $\Omega$  with better than 15-dB return loss even up to 40 GHz (unactuated state). This is due to the low off-capacitance of this switch, which is on the order of 25–50 fF. The insertion loss and return loss as a function of frequency are shown in Fig. 6. The isolation and return loss of the switch in the on-state (actuated) is shown in Fig. 7. The isolation of the switch is approximately 15 dB at 10 GHz and 35 dB at 35 GHz, which are sufficient for switching RF signals.

The turn-on and turn-off switching waveforms for the membrane switch are shown in Fig. 8. The measured switching

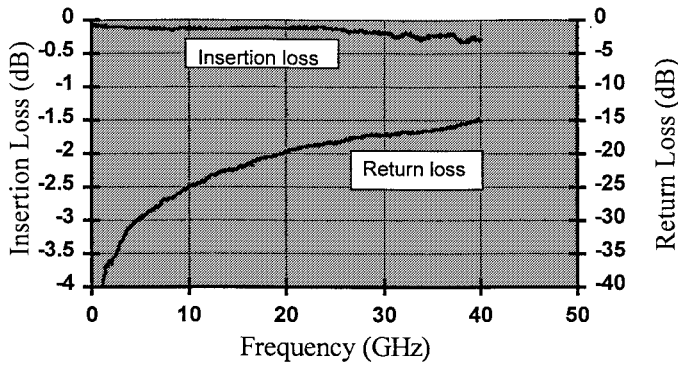


Fig. 6. Switch insertion loss and return loss as a function of frequency (up position).

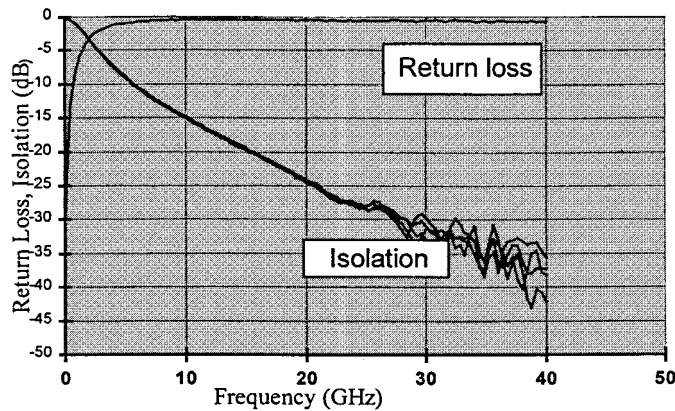


Fig. 7. Switch isolation and return loss as a function of frequency (down position).

actuation time is about  $5.3 \mu\text{s}$ , while the measured switching up time is  $3.5 \mu\text{s}$ . It should be noted that these waveforms were taken without any dielectric charging present. When actuating switches on and off, it is possible for the high electric field across the thin dielectric to cause charges to tunnel into the dielectric and become trapped. These charges screen the applied electric field, causing the switches to need higher switching voltages and to have difficulties switching using unipolar dc control voltages. Techniques to mitigate this charging are an area of ongoing research.

To accurately evaluate switching speed, a nonlinear dynamic model that captures the effects of electrostatics, deformation, residual stress, inertia, damping, Van der Waals force, impact, contact, and air dynamics is essential. There is neither a closed-form solution nor a simulation tool for MEMS dynamics at present. As a first-order approximation, the switching speed of these devices is determined by the mechanical primary natural frequency of the devices. Finite-element analyses using ABAQUS [12] show that the primary frequencies of these devices ranged from 56 to 150 kHz depending on the magnitude of residual stresses. A rule of thumb for switching speed is that the switches will change state (between up and down) in  $1/4$  of a cycle of the primary frequency. This puts the switching speed (up or down) in the  $1.67\text{--}4.5 \mu\text{s}$  range.

Switch lifetime was tested by the application of a continuous train of control pulses at repetition rates between 500 Hz and

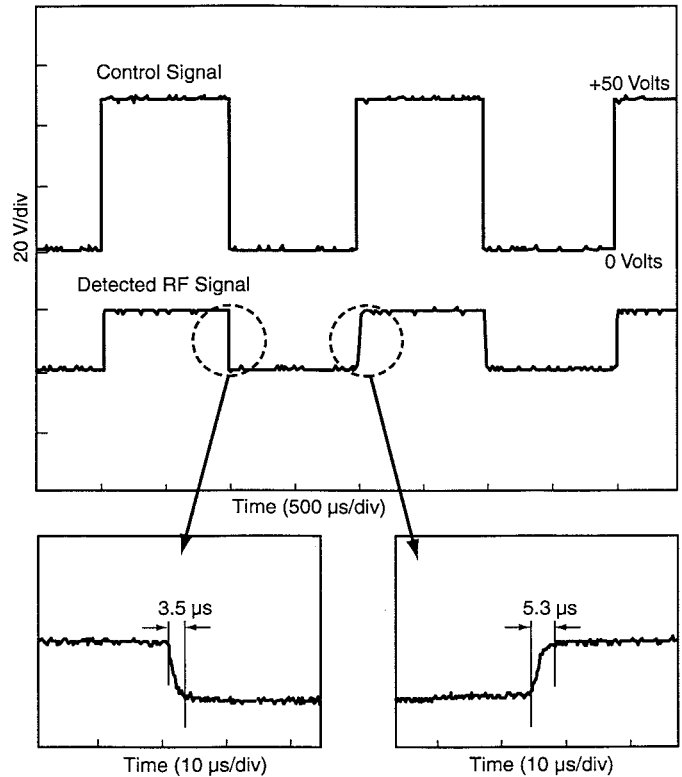


Fig. 8. Switching speed measurement results.

5 KHz. The membrane went through 500 million switching cycles and no mechanical failures were detected.

The actuation voltage of the capacitive switches is about 50 V. The actuation voltage depends primarily on the spring constant of the mechanical system of the membrane. The mechanical position of the membrane is determined by the applied voltage, the membrane geometry, the membrane material properties, and the gap height between the membrane and the bottom electrode. A first-order solution of the pull-down voltage ( $V_p$ ) can be calculated by the following equation [9]:

$$V_p = \sqrt{\frac{8K_s g_o^3}{27\epsilon}} \quad (4)$$

where  $K_s$  is the spring constant of the mechanical system,  $g_o$  is the initial gap between two capacitor plates, and  $\epsilon$  is the permittivity of medium surrounding the conductors. This single degree freedom model only gives a first-order prediction of pull-down voltage. An improved 2-D model also has its limitations [10]. The dimensions of membrane switch described in this paper do not satisfy the requirements set by this model. Therefore, the pull-down voltage was computed using a full 3-D numerical simulation commercial software [11]. With a Young's modulus of 70 MPa for bulk aluminum, a residual stress in the membrane of 120 MPa, the estimated pull-down voltage is about 56 V, which is close to the test results.

## VI. CONCLUSIONS

Micromechanical membrane switches for microwave applications were designed, fabricated, and tested. The switches

show excellent results: low loss and high isolation in the frequency range of 10–35 GHz. These switches have significant advantages compared to typical FET and p-i-n diode switches and other MEMS switch topologies. These devices offer the potential for building a new generation of low loss high-linearity microwave circuits for a variety of phased antenna arrays for radar and communications applications.

#### ACKNOWLEDGMENT

The authors would like to thank T. Session, T. Smith, and S. Harley for their support.

#### REFERENCES

- [1] K. E. Petersen, "Micromechanical membrane switches on silicon," *IBM J. Res. Develop.*, vol. 23, no. 4, pp. 376–385, July 1979.
- [2] J. J. Yao and M. F. Chang, "A surface micromachined miniature switch for telecommunications applications with single frequencies from DC up to 4 GHz," in *Proc. Transducers'95*, June 1995, pp. 384–387.
- [3] S. Zhou, X. Sun, and W. N. Carr, "A micro variable inductor chip using MEMS relays," in *Proc. Transducers'97*, June 1997, pp. 1137–1140.
- [4] L. E. Larson, R. H. Hakett, M. A. Melendes, and R. F. Lohr, "Micromachined microwave actuator technology—A new tuning approach for microwave integrated circuits," in *IEEE Microwave and Millimeter-Wave Monolithic Circuit Symp.*, 1991, pp. 27–30.
- [5] C. Goldsmith, T. H. Lin, B. Powers, W. R. Wu, and B. Norvell, "Micromechanical membrane switches for microwave applications," in *IEEE Microwave Theory Tech. Symp.*, May 1995, pp. 91–94.
- [6] C. Goldsmith, J. Randall, S. Eshelman, T. H. Lin, D. Denniston, S. Chen, and B. T. H. Norvell, "Characteristics of micromachined switches at microwave frequencies," in *IEEE Microwave Theory Tech. Symp.*, May 1996, pp. 1141–1144.
- [7] R. H. Caverly, "Distortion in off-state arsenide MESFET switches," *IEEE Trans. Microwave Theory Tech.*, vol. 41, pp. 2295–2302, Dec. 1993.
- [8] K. W. Kobayashi, A. K. Oki, D. K. Umemoto, S. K. Z. Claxton, and D. C. Streit, "Monolithic GaAs HBT p-i-n diode variable gain amplifiers, attenuators, and switches," *IEEE Trans. Microwave Theory Tech.*, vol. 41, pp. 1323–1328, Aug. 1993.
- [9] P. Osterberg, H. Yie, X. Cai, J. White, and S. Senturia, "Self-consistent simulation and modeling of electrostatically deformed diaphragms," in *Proc. MEMS'94*, Osio, Japan, Jan. 1994, pp. 28–32.
- [10] P. M. Osterberg, "Electrostatically actuated microelectromechanical test structures for material property measurement," Ph.D. dissertation, Massachusetts Inst. Technol., Cambridge, MA, 1995.
- [11] IntelliCAD Version 3.5, IntelliSense Corporation, 16 Upton Drive, Wilmington, MA 01887.
- [12] ABAQUS/Standard Version 5.7, Hibbitt, Karlsson, & Sorensen, Inc., 1080 Main Street, Pawtucket, RI 02860-4847.



**Z. Jamie Yao** received the Ph.D. degree from the School of Materials Science and Engineering, Georgia Institute of Technology, Atlanta, in 1995.

She was a Post-Doctoral Research Associate at the School of Electrical Engineering, Cornell University, Ithaca, NY, for about a year. Her research emphasis was on silicon bulk micromachining. She is currently with the Applied Research Laboratories, Raytheon Systems Company (formerly the Central Research Laboratory of Texas Instruments), Dallas, TX. Her research interests include design, fabrication, and characterization of microelectromechanical systems.



**Shea Chen** received the B.Sc. degree in mechanical engineering from Tamkang University, Taiwan, R.O.C., in 1976, the M.Sc. degree in mechanical engineering from the University of Texas at Arlington, in 1981, and the Ph.D. degree in engineering mechanics from the Southern Methodist University, Dallas, TX, in 1991.

He was with PECL, R.O.C., performing structural analysis and the Southern Methodist University, where he researched numerical simulations of incompressible free-surface fluid flows. Since 1995, he has been with Raytheon Systems, Dallas, where he is an RF/Microwave Mechanical Engineer. His current interests are thermal cycling and vibration failures in electronic equipment, probability of failure of brittle components and devices, and mechanical design and analysis of microelectromechanical switches.

Dr. Chen is a member of ASME.

**Susan Eshelman** received the B.A. degree in chemistry from Austin College, Sherman, TX, in 1988 and the M.S. degree in chemistry at the University of Texas at Dallas in 1992.

She completed an internship on planarization of semiconductor devices at Texas Instruments. She joined the photonics branch of Texas Instruments' Central Research Lab in 1994 and developed processes for fabricating optical waveguides and micromachined optical switches. These optical switches formed the mechanical basis of the current work on RF switches, although processes continue to improve and change as the designs are modified. She continued this work in collaboration with Stanford University and Texas Instruments. Currently, she continues to contribute to the process development and fabrication of devices in the RF MEMS branch of the RF Microwave Division of Raytheon Systems, Dallas.



**David Denniston** (A'96) received the B.S. degree in applied mathematics at the University of Texas at Dallas in 1996. He is currently working toward the Master's degree in electrical engineering at the University of Texas at Dallas.

He joined the Antenna Lab, Texas Instruments, in 1986 as an Engineering Technician while working on his B.S. degree part time. Later he transferred to the Advanced Phased Array Components section of the Microwave Laboratory. He was involved with system design and testing of the  $Ku$ -band transmit phased array for the NASA ACTS satellite KaMIST airborne terminal testbed. His current assignment includes research and design of  $Ku$ - and  $Ka$ -band monolithic microelectromechanical systems (MEMS) phase shifters for use in phased array modules. He is the coauthor of several papers on MEMS for RF and millimeter-wave switching.

Mr. Denniston has been a past Program Chairman and present Treasurer for the Dallas Chapter of the MTT Society over the last two years.



**Chuck Goldsmith** (SM'94) was born in Chicago, IL, in March 1958. He received the Bachelor's and Master's degrees in electrical engineering from the University of Arizona, Tucson, in 1980 and 1982 and the Ph.D. degree from the University of Texas at Arlington in 1995.

Since 1986, he has been involved in the design and development of microwave and millimeter-wave circuits and subsystems for the Raytheon Systems Company (formerly the Defense Electronics Group of Texas Instruments), Dallas, TX. Currently, he is involved in the development of RF MEMS for numerous receiver and antenna applications.